Journal of Alasmarya University: Basic and Applied Sciences
Vol. 6, No. 5, December 2021, Special Issue for Forth Conference on Engineering Science and Technology (CEST-2021)
مجلة الجامعة الأسمرية: العلوم الأساسية والتطبيقية
المجلد 6 ،العدد 5، ديسمبر 2021، عدد خاص بالمؤتمر الرابع للعلوم الهندسية والتقنية (CEST-2021)

Enhanced Dct Image Watermarking Scheme Based on Zonal Sampling Algorithm Applied With Sspce Contour Extraction, Ramer and Adaptive Triangle Contour Compression Methods

Majdi Farag Mohammed El Bireki[1,*], Ali Abdrahman M Ukasha[2], Jamal Ali Ramadan Dofan[3], M. F. L. Abdullah[4]

[1]*Department of Electrical and Electronic Engineering, Higher Institute of Professions Over all, Tamazawa, Libya, majdi_elbreki@yahoo.com*

[2]*Department of Electrical and Electronic Engineering, Sebha University, Sebha, Libya, ali.ukasha@sebhau.edu.ly*

[3]*Department of Electrical and Electronic Engineering, Gharian University, Gharian, Libya, jardgsm@gmail.com*

[4]*Faculty Electrical & Electronic Engineering, Universiti Tun Hussein Onn Malaysia (UTHM), faiz@uthm.edu.my*

ABSTRACT

This paper proposes an image watermarking scheme based on DCT transform and selected zonal sampling algorithms. The scheme used LPF and HPF transform coefficients in a certain geometric zone of the original image are retained. All the rest of the parameter is set to zero (0), quantized and transmitted where the watermark will be embedded. In order to test robustness, some attacks are performed. However, prior to the watermark extraction process, the attacked watermarked image will be subdued into contour processing methods using Single Step Parallel Contour Extraction, Ramer and Adaptive Triangle algorithms. The proposed method for contour compression will help enhance image recognition, security and especially where time (speed) is an essential factor. The results show that the proposed watermarking method is robust and secure against various signal/image processing attacks with PSNR values of approximately 35 dB with NCC values of 0.60 and above. In addition, experimental results from contour compression indicate that the proposed Adaptive Triangle method has a high compression ratio without significant visible distortion.

***Keywords**:*
Watermarking.
Contour.
DCT.
Ramer.
Adaptive Triangle.

**Corresponding Author Email: majdi_elbreki@yahoo.com*

1 INTRODUCTION

An image is defined as a representation, likeness or imitation of an object or thing; it is a vivid or graphic description or something to represent something else [1] which can be stored in any representation, provided there is an algorithm that can convert it to a form usable by a display [2]. As technology in a rapid speed has developed in the area of software and internet, storing (digital) information is no longer safe for they can be easily copied, stolen and distributed. Traditional encryption technology somehow is deficient, giving way to the emergence of digital watermarking techniques. Contour extraction (using SSPCE) and compression (using Ramer) from digital medical image are used as in [29,30]. Recently, Arabic & English binary contours are compressed using new approaches as in [31,32]. These digital watermarking techniques hide a special or distinct message in images, video, songs, texts and any multimedia data. However, digital watermarking techniques must also meet the requirement of imperceptibility, robustness and security [3,4] in order to be effective. For instance, the imperceptibility and the robustness requirements are two conflicting factors. Therefore, from a signal processing point of view, imperceptibility limits the strength of the embedded watermark. On the other hand, it is important to encode a relatively strong watermark for it to be resistant to content manipulation and attacks. A similar conflict may hold for the requirements of information capacity and efficiency. Hence, certain trade-offs (or compromises) are involved in the design of an effective watermarking system. Digital watermarking is essential because it aims to establish ownership [5] of the content i.e. image, a fingerprint to avoid unauthorized duplication and distribution of publicly available media content, for authentication and integrity verification purposes, Furthermore, watermark is added as usage control in order to limit the number of copies created, for content labeling and for content protection. Digital watermarks can be applied in copyright protection systems which are intended to prevent or determine unauthorized copying of digital media [6], source tracing or as broadcast monitoring application [7]. Unfortunately, there is not a universal watermarking technique to satisfy all these purposes [8]. The content in the environment that it will be used determines the digital watermarking technique.

Watermarking algorithms can be divided into two major categories: spatial and frequency domains. Spatial domain algorithms such as LSB [9], [10], Predictive coding, correlation-based techniques and patchwork techniques [11] have the advantages of fast and simple operations, utilizing the human visual system but the robustness, image quality and data payload have been greatly compromised. Frequency domain algorithms, on the other hand, first analyses a given signal whose structure and features are better understood by transforming the data into another domain [12,13-15]. There are several transforms available like the Fourier transform, Hilbert transform, wavelet transform, etc. In [15], discrete cosine transform (DCT) and discrete wavelet transform (DWT) are used for embedding and extracting watermark and concluded that DWT gives better image quality than DCT. However, DCT has its advantages too. It has a special property that most of the visually significant information of the image is concentrated in just a few coefficients of the DCT referred to as ‘energy compaction property’. Many DCT based digital image watermarking algorithms are developed because of this property [16]. DCT transforms a signal from a spatial representation into frequency representation [17]. Lower frequencies are more obvious in an image than higher frequencies. Therefore, if an image is transformed into its frequency components and throw away a lot of higher frequency coefficients, the amount of data required to describe the image can be reduced without sacrificing too much image quality. DCT has the property that, for a typical image, most of the visually significant information about the image is concentrated in just a few coefficients of the DCT. Therefore, for this reason, the DCT is often used in image compression applications [12].

2 WATERMARKING METHODOLOGY

2.1 Block diagram of the proposed enhanced digital watermarking scheme

Watermarking schemes generally have three parts: the watermark, the embedding and extraction. In this section, the block diagrams of the proposed method are shown in Fig. 1a and Fig. 1b. The watermarking algorithm has two stages. In the first stage, the watermark is embedded in the original image using the proposed enhanced methods DCT for image compression and zonal sampling, to embed the watermark in the most secure position. A key is used during the embedding process. Then, DCT process is inverted to obtain the watermarked image. It is then transmitted to the receiver which has the watermarked image. This watermarked image will be tested for its robustness by applying various image processing attacks. In the second stage, the receiver then extracts the attacked host image which has been watermarked, using the inverse algorithm process performed in the first stage. The proposed watermarking scheme is performed using MATLAB software.

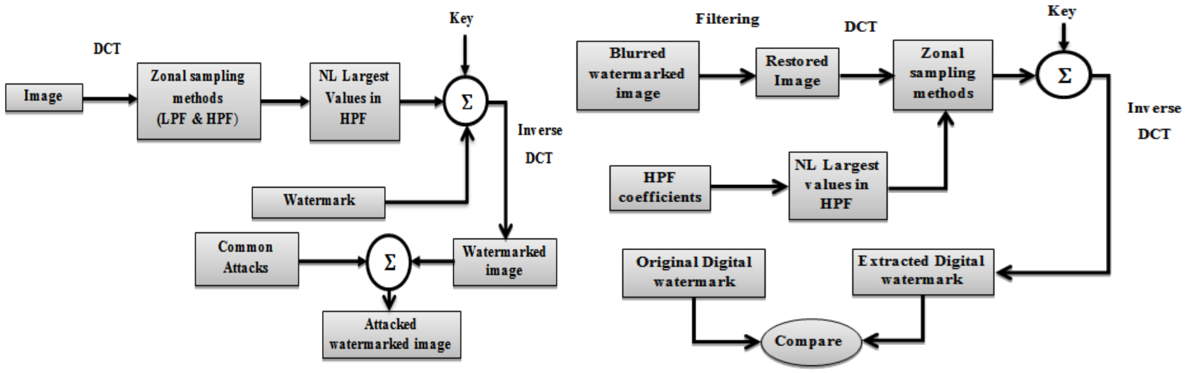

a. Embedding algorithm b. Extraction algorithm

Figure 1. The proposed enhanced watermarking algorithm

2.2 Embedding process

The original gray level image is compressed first using DCT method with the forward formula (1) [18].

$$K_{pq} = \alpha_p \alpha_q \sum_{m=p}^{M-1} \sum_{n=q}^{N-1} A_{nm} \cos\frac{\pi(2m+1)p}{2M} \cos\frac{\pi(2n+1)q}{N} \quad (1)$$

Where, $0 \le p \le N-1$, $0 \le q \le N-1$,

$$\alpha_p = \begin{cases} \frac{1}{\sqrt{N}} & ,p=0 \\ \sqrt{\frac{2}{N}} & ,1 \le p \le N-1 \end{cases}, \alpha_q = \begin{cases} \frac{1}{\sqrt{N}} & ,q=0 \\ \sqrt{\frac{2}{N}} & ,\ 1 \le q \le N-1 \end{cases}$$

Where M and N are the rows and columns of an image. Then, zonal sampling is performed.

2.3 Zonal sampling

In the encoding/embedding process, transform coefficients are stored. It is the art of choosing the right place to embed the data. Zonal sampling refers to the sampling scheme where transform coefficients in a certain geometric zone are retained and all the rest is set to zero (0). The coefficients that are in the zone are then quantized and transmitted. An inverse transform is performed on the quantized coefficients in order to recover the original image. For a fixed bit rate, the performance, such as image quality and mean square error, will thus depend on the transform used, size of block, geometric shape and size of the sampling zone and quantization bit allocation of the transform coefficients [19]. In this paper, two geometric zones are selected to retain the transform coefficients in embedding the watermark data. The rest of the transform coefficients of the host image must be set to zero. In zonal sampling algorithm 1, a square block in the upper left corner N*M of the host image (shadow region, Low Pass Filters) is the chosen region where the transform coefficients are set to zero. The transform coefficients outside the shadow region (High pass Filters) will be retained and will be used to embed data as shown in Fig. 2a and Fig. 3a; while zonal sampling algorithm II uses a triangular block in the upper left corner N*M of the host image as illustrated in Fig. 2b and Fig. 3b. After finding the index of the N largest coefficient values of the HPF, the watermark can then be embedded with the use of a key. The inverse process, IDCT is performing using formula (2) in order to obtain the watermarked image [18].

$$A_{pq} = \sum_{m=p}^{M-1} \sum_{n=q}^{N-1} \alpha_p \alpha_q K_{nm} \cos\frac{\pi(2m+1)p}{2M} \cos\frac{\pi(2n+1)q}{N} \tag{2}$$

Where, $0 \le p \le N-1$, $0 \le q \le N-1$,

$$\alpha_p = \begin{cases} \frac{1}{\sqrt{N}} & ,p=0 \\ \sqrt{\frac{2}{N}} & ,1 \le p \le N-1 \end{cases}, \alpha_q = \begin{cases} \frac{1}{\sqrt{N}} & ,q=0 \\ \sqrt{\frac{2}{N}} & ,\ 1 \le q \le N-1 \end{cases}$$

Where M and N are the rows and columns of an image.

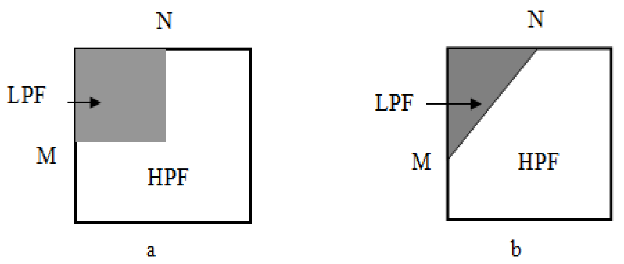

Figure 2. Zonal sampling (a) Algorithm I (b) Algorithm II

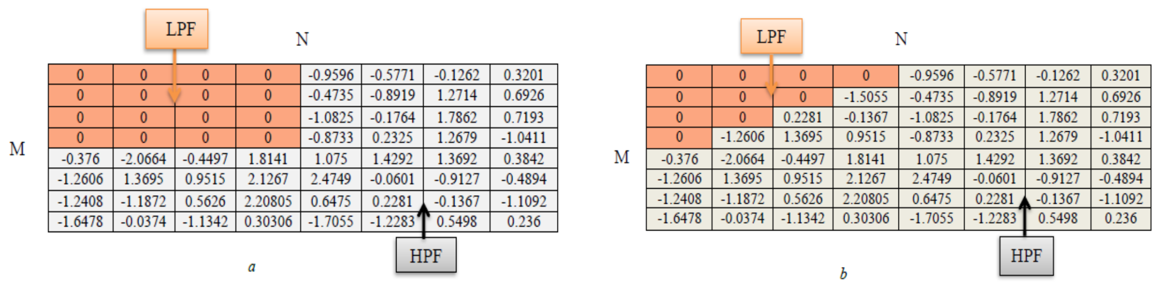

0	0	0	0	-0.9596	-0.5771	-0.1262	0.3201
0	0	0	0	-0.4735	-0.8919	1.2714	0.6926
0	0	0	0	-1.0825	-0.1764	1.7862	0.7193
0	0	0	0	-0.8733	0.2325	1.2679	-1.0411
-0.376	-2.0664	-0.4497	1.8141	1.075	1.4292	1.3692	0.3842
-1.2606	1.3695	0.9515	2.1267	2.4749	-0.0601	-0.9127	-0.4894
-1.2408	-1.1872	0.5626	2.20805	0.6475	0.2281	-0.1367	-1.1092
-1.6478	-0.0374	-1.1342	0.30306	-1.7055	-1.2283	0.5498	0.236

0	0	0	0	-0.9596	-0.5771	-0.1262	0.3201
0	0	0	-1.5055	-0.4735	-0.8919	1.2714	0.6926
0	0	0.2281	-0.1367	-1.0825	-0.1764	1.7862	0.7193
0	-1.2606	1.3695	0.9515	-0.8733	0.2325	1.2679	-1.0411
-0.376	-2.0664	-0.4497	1.8141	1.075	1.4292	1.3692	0.3842
-1.2606	1.3695	0.9515	2.1267	2.4749	-0.0601	-0.9127	-0.4894
-1.2408	-1.1872	0.5626	2.20805	0.6475	0.2281	-0.1367	-1.1092
-1.6478	-0.0374	-1.1342	0.30306	-1.7055	-1.2283	0.5498	0.236

Figure 3. Zonal sampling (a) Algorithm I (b) Algorithm II

2.4 Extraction process

This method is used to retrieve the watermark which was inserted in the original image. The attacked watermarked image will be restored by first applying a filtering process. Then, the restored image will be transformed by applying DCT again and then determine the N largest coefficients of the HPF. After that, inverse transform IDCT will be applied to obtain the extracted watermark. The extracted watermark is then compared with the original watermark image. Zonal sampling is used to separate Low Pass Filter and High Pass Filter coefficients. LPF coefficients will be used for image compression while the remaining HPF coefficients will be used in the contour reconstruction stage. The two spectral sub-images are obtained using the low and high-pass filters after the zonal sampling procedures (in both algorithms I and II).

2.5 Contour compression processing

This paper has integrated contour processing which is performed after the embedding process; it is aimed to test a new method for contour compression known as the Adaptive Triangle method. After obtaining the watermarked image, it undergoes various attacks. One of the applied attacks is blurring. From this point, threshold is applied to obtain a binary image of the attacked watermarked image. In order to extract its contours, SSPCE method is used. Then, these contours are compressed using the Ramer/Adaptive Triangle method. The block diagram of this technique is shown in Fig.4

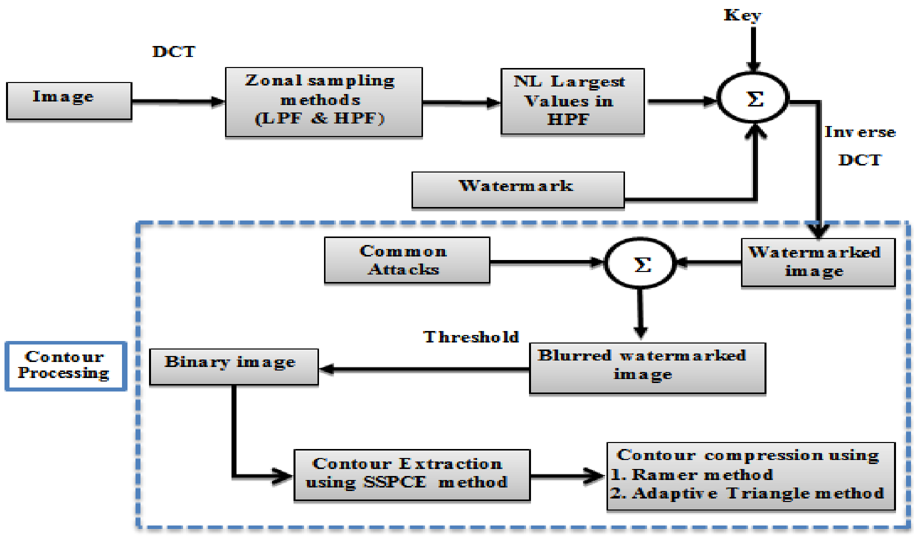

Figure 4. Block diagram of contour extraction using SSPCE and compression using Ramer and Adaptive Triangle methods

3.5.1 Single Step Parallel Contour Extraction (SSPCE) Algorithm:

The contour data for the proposed algorithm is extracted from black-white images (which can be derived from colour or gray images by conversion) using a well-known method of contour extraction called SSPCE. There are two methods that use a 3×3 pixels window structure to extract the object contours using the central pixel to find the possible edge direction, which connect the central pixel with one of the remaining pixels surrounding it. The first one uses 8-connectivity scheme between pixels using the 8-Directional Freeman chain coding scheme to distinguish all eight possible line segments connecting the nearest neighbours. The second algorithm uses the 4-connectivity scheme between pixels using 4-Directional Freeman chain coding scheme to distinguish all four possible line segments. This paper uses the first mentioned method.

The following three stages are required for the extraction procedure:

Stage 1: Put zeros to the border line.

Stage 2: Extract contours by applying 8-directional chain-code. The extracted edge code is represented by 2^k (k: 0-7), while b(i, j) represents the binary value of a pixel point (i, j) and are calculated using pseudocodes .

Stage 3: Sort and optimize [20, 21, 28].

3.5.2 Contour compression using the Ramer method:

The algorithm is based on the maximum distance of the curve from the approximating polygon and this distance is used as the fit criterion. The algorithm produces a polygon with a small number of edges for arbitrary two-dimensional digitized curves. The segment of the curve is approximated using a straight-line segment connecting its initial and terminus. If the fit criterion is not fulfilling, the curve segment is terminated into two segments at the curve point most distant from the straight-line segment. This loop is repeated until each curve segment can be approximated by a straight-line segment through its endpoints. The termini of all these curve segments then are the vertices of a polygon that satisfy the given maximum-distance approximation criterion [22, 23, 24] as shown in Fig. 5. This distance is compared using the given threshold as formulated in 3 [22]:

$$d_{\max} > th \qquad (3)$$

Where SP is the starting point; EP is the ending point; d_{max} is the maximum distance from (SP-EP) line to the contour curve; th is threshold. This loop is repeated until each curve segment can be approximated by a straight-line segment through its endpoints. The termini of all these curve segments then are the vertices of a polygon that satisfy the given maximum-distance approximation criterion. This type of polygonal curve representation exhibits two important disadvantages. First the polygons contain a very large number of edges and, therefore, are not in as compact a form as possible. Second, the length of the edges is comparable in size to the noise introduced by quantization.

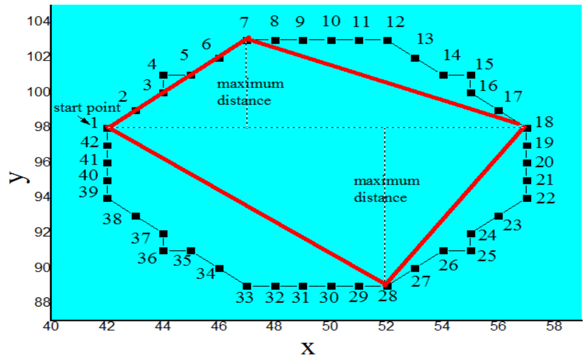

Figure 5. Curve approximation using the Ramer method

3.5.3 Contour compression using Adaptive triangle method:

Adaptive Triangle method is perform by choosing two points on the contour curve and computes the maximum distance from contour curve to the straight line that connects them as shown in Fig.6. This distance is compared using the given threshold as formulated in 4:

$$d_{\max} > th_1 \qquad (4)$$

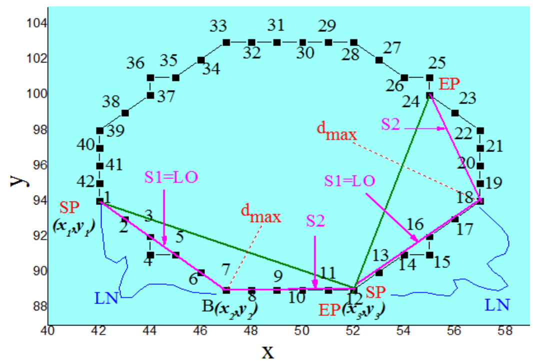

Figure 6. Curve approximation using Adaptive triangle method

VA is the sequence of indices of the final vertices; CC is the sequence of the input for the contour; SP is the starting point; EP is the ending point; d_{max} is the maximum distance from (SP- EP) line to the contour curve; L is the input contour length and (f) is the length between each two points, S1 is length of first segment of vertex point, S2 is length of second segment of vertex point, LN is real distance between start and end point of vertex segment, LO is direct distance between start and end point of vertex segment, ff is segment length of the vertex point , th_1 is Threshold1 and th_2 is Threshold2. If the ratio between the direct distance and the real distance is smaller than the second threshold [22]:

$$\mathrm{LO/LN} > \mathrm{th}_2 \tag{5}$$

This step is to show what happens in case the ratio value exceeds the threshold value. If the ratio exceeds the second threshold th2 value, then no edge points between the starting and ending points of the triangle will be stored.

2.6 Research parameter measurement

Robustness: Watermarking method's robustness is assessed by applying attacks (geometrical, noise, image compression, etc.) on the watermarked image and evaluates the similarity of the extracted watermark to the original watermark. The Normalized Correlation Coefficient is expressed in the following equation 6 [25]:

$$\mathbf{NCC} = \frac{\sum_i \sum_j [\mathbf{W(i,j)}.(\mathbf{W'(i,j)}]}{\sum_i \sum_j [\mathbf{W(i,j)}]^2} \tag{6}$$

Where $\mathrm{W(i,j)}$ = original watermark; $\mathrm{W'(i,j)}$ = extracted watermark after transformation. Its value should be closed to 1 or 1 for a watermark to be considered robust, meaning, high similarity is achieved between the extracted watermark and the original watermark.

Imperceptibility: The original image and the watermarked image' quality (statistical difference) is measured using peak signal-to-noise ratio (PSNR). The PSNR between the original and reconstructed images is expressed in the equation 7 [25]:

$$\mathbf{PSNR(I,\tilde{I}) = 10\log_{10}\frac{(L-1)^2}{MSE(I,\tilde{I})}} \tag{7}$$

Where L = grey-level number; I = original mage; $\tilde{I}$= watermarked image.

Quality measurement: In order to measure the quality of an approximation during the approximating procedure, mean square error (MSE) and signal-to-noise ratio (SNR) criteria are used 8 [22]:

$$\mathrm{MSE} = \frac{1}{\mathrm{L_{CC}}} \sum_{i=1}^{\mathrm{L_{CC}}} \mathrm{d}_i^2 \tag{8}$$

Compression ability: In order to evaluate the compression ability of the scheme (i.e. zonal sampling), the following compression ratio is used 9 [22]:

$$\mathrm{CR} = \frac{\mathrm{NOZ} * 100\%}{(\mathrm{n} * \mathrm{m})} \tag{9}$$

Where NOZ is number of the zero coefficients in the spectral domain and the (n, m) are the number of rows and column of the image. Bit per pixel (BPP) is expressed in 10 [22]:

$$\text{BPP} = \frac{\text{S}\times 8}{(\text{n}\times\text{m})} \tag{10}$$

Where: S = Coefficients number in the desired zonal used as LPF filter; 8 = Means each pixel represented by eight bit; n × m = size of the image.

3 EXPERIMENTAL RESULTS

3.1 Experimental results of various host images using DCT with zonal sampling I & II

In this section, tests were conducted to evaluate the imperceptibility and robustness of the proposed method. The test images have 512*512 size; zonal sampling I size is set to N=M=66 and zonal sampling II is set to N=M=47. The size of the watermark UTHMFKEE is 141*157. The test images are shown in Fig. 7(a-f). A new watermark is used as shown in Fig. 8. Table 1 - Table 3, present the results of watermarked images, attacked watermarked images and the extracted watermark in zonal sampling I while zonal sampling II experimental results are shown from Table 4 - Table 6. These tables display the test results of the extracted watermark in several attacks. It can be seen that different parameters of attacks are chosen to achieve a PSNR of about 35 dB for the watermarked images and the NCC of the extracted watermark should at least be 0.60 and above in order to be considered robust. It is observed that at such PSNR, the watermarked images are almost indistinguishable from the original image to the human eyes.

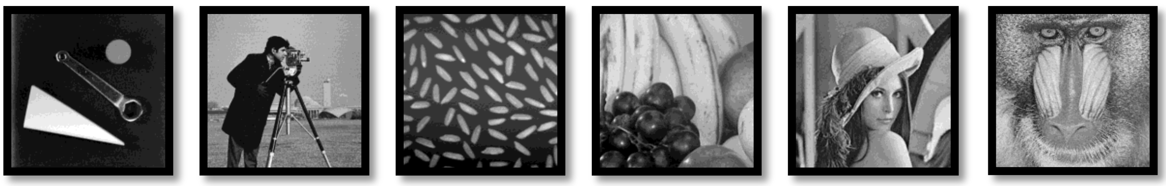

a b c d e f

Figure 7. Various test host images (a) Tools (b) Cameraman (c) Rice (d) Fruit (e) Lena (f) Baboon

Figure 8. The original watermark

Table 1. DCT with zonal sampling I experimental results without attack, salt and peppers and JPEG attacks

Attack \ Images		Watermarked Image	Attacked Watermarked Image	Extracted Watermark Image	
No Attack	Measurements	Tools			
	MSE	1.5854	1.5854	-	
	PSNR [dB]	46.1294	46.1294	-	
	NCC	-	-	1	
Salt & Pepper 10%	Measurements	Cameraman			
	MSE	7.5802	18.8589	-	
	PSNR [dB]	40.2051	35.3560	-	
	NCC	-	-	0.7116	
JPEG 65%	Measurements	Fruit			
	MSE	2.9400	5.8007	-	
	PSNR [dB]	43.4474	40.4960	-	
	NCC	-	-	0.8050	

Table 2. DCT with zonal sampling I experimental results with Gaussian noise, blurring attacks motion and LoG

Attack \ Images			Watermarked Image	Attacked Watermarked Image	Extracted Watermark Image	
Gaussian		Measurements	Cameraman			
Mean 0	Var 0.001	MSE	7.5802	33.8060	-	
		PSNR [dB]	40.2051	32.8160	-	
		NCC	-	-	0.8195	
Motion		Measurements	Rice			
Len 41	Theta 13	MSE	1.9927	558.8210	-	
		PSNR [dB]	45.1363	20.6581	-	
		NCC	-	-	0.9972	
LoG		Measurements	Lena			
Hsize [3 3]	Sigma 5	MSE	3.2338	1.7607e+004	-	
		PSNR [dB]	42.1833	5.6739	-	
		NCC	-	-	0.8563	

Table 3. DCT with zonal sampling I experimental results with sharpening, LPF and median filter

Attack \ Images		Watermarked Image	Attacked Watermarked Image	Extracted Watermark Image	
Sharpened $\begin{bmatrix} 0 & -1 & 0 \\ -1 & 5 & -1 \\ 0 & -1 & 0 \end{bmatrix}$	Measurements	Baboon			
	MSE	10.6102	1.1958e+003	-	
	PSNR [dB]	38.1325	17.3541	-	
	NCC	-	-	0.9982	
LPF 1/50* ones[7 7]	Measurements	Tools			
	MSE	1.5854	18.8939	-	
	PSNR [dB]	46.1294	35.3676	-	
	NCC	-	-	0.6086	
Median Filter [3 3]	Measurements	Fruit			
	MSE	2.9400	2.9400	-	
	PSNR [dB]	43.4474	42.5381	-	
	NCC	-	-	0.8719	

Table 4. DCT with zonal sampling II experimental results without attack, salt and peppers and JPEG attacks

Attack \ Images		Watermarked Image	Attacked Watermarked Image	Extracted Watermark Image	
No Attack	Measurements	Fruit			
	MSE	2.9134	2.9134	-	
	PSNR [dB]	43.4867	43.4867	-	
	NCC	-	-	1	
Salt & Pepper 8%	Measurements	Baboon			
	MSE	10.5802	24.6459	-	
	PSNR [dB]	38.1404	34.2221	-	
	NCC	-	-	0.6137	
JPEG 75%	Measurements	Lena			
	MSE	4.2840	8.3617	-	
	PSNR [dB]	42.1484	38.9079	-	
	NCC	-	-	0.9662	

Table 5. DCT with zonal sampling II experimental results with Gaussian noise, blurring attacks motion and LoG

Attack \ Images			Watermarked Image	Attacked Watermarked Image	Extracted Watermark Image	
Gaussian		Measurements	Cameraman			
Mean 0	Var 0.001	MSE	7.4195	33.7428	-	
		PSNR [dB]	40.2501	32.8299	-	
		NCC	-	-	0.8184	
Motion		Measurements	Rice			
Len 21	Theta 11	MSE	1.9996	154.6105	-	
		PSNR [dB]	45.1214	26.2384	-	
		NCC	-	-	0.9980	
LoG		Measurements	Tools			
Hsize [3 3]	Sigma 5	MSE	1.5874	5.9392e+003	-	
		PSNR [dB]	46.1240	10.3935	-	
		NCC	-	-	0.9982	

Table 6. DCT with zonal sampling II experimental results with sharpening, LPF and median filter attacks

Attack \ Images		Watermarked Image	Attacked Watermarked Image	Extracted Watermark Image	
Sharpened $\begin{bmatrix} 0 & -1 & 0 \\ -1 & 8 & -1 \\ 0 & -1 & 0 \end{bmatrix}/4$	Measurements	Lena			
	MSE	4.2840	12.8926	-	
	PSNR [dB]	42.1484	37.0274	-	
	NCC	-	-	0.9712	
LPF 1/9* ones[3 3]	Measurements	Cameraman			
	MSE	7.4195	23.6108	-	
	PSNR [dB]	40.2501	34.3997	-	
	NCC	-	-	0.9585	
Median Filter [3 3]	Measurements	Tools			
	MSE	1.5874	1.7096	-	
	PSNR [dB]	46.1240	45.8020	-	
	NCC	-	-	0.8928	

The proposed watermarking method will undergo enhanced testing. First with no attack giving a perfect correlation value of 1. Noise addition attack (Salt and peppers, Gaussian noise), Filtering attack (Gaussian LPF, median filters), Various attack (sharpening, blurring motion), LoG and JPEG Compression are among the few image processing attacks used to test the robustness of the scheme. The results are shown in Tables 1-6. According to the results obtained from Tables 1-6, the proposed watermarking method is robust against various blurring attacks. The extracted watermark is near identical specially in motion blurring with a very high PSNR value after extraction as the PSNR value is always greater than 35 dB (without attack) and there is high correlation after all attacks have been applied. These results show that the watermarked document is visually near identical to the original image. In addition, the simulation results indicate that the proposed watermarking method is robust against signal processing attacks such as JPEG compression, salt and peppers, adding blurring attacks like Gaussian, motion attack such as blurring, LoG, sharpening, low pass filtering and median filtering. A correlation value above 0.60 is considered robust after watermark extraction. However, the proposed watermarking method shows vulnerability to salt and peppers noise. Nevertheless, correlation coefficient is still above 0.60 which means that the extracted watermark nearly resembles the original watermark after attacks are applied.

3.2 Enhanced watermarking method using DCT with zonal sampling I and II algorithms against other related work methods.

The proposed method is tested on gray level test image Lena of size 512*512 pixels with a watermark image of size 64*64 pixels, a logo taking the alphabets ‘JNTUACEA’ as shown in Fig. 9(a-b). In this experiment, six different image processing attacks are used. The comparative results are measured by its normalized cross correlation (NCC) values to prove robustness against various attacks mentioned. Image processing attacks applied to the watermarked image include JPEG with QF= 50 and a salt and peppers noise of 1%. All the edges in the image are enhanced in sharpening attack. The watermarked image is passed through a low pass filter wherein median filter is applied for filtering attacks. In this attack, the image is smoothened, and from this, watermark image is extracted. Finally, blurring motion attack is applied to test the robustness of the scheme.

(a) *(b)*

Figure 9. Original host image (a) Lena and (b) Watermark “JNTU ACEA”

The results in Table 7 and Fig. 10 show the NCC values of the test image after watermark embedding and extraction processes are performed using the proposed method and compared with FIS method [26]. In most results, the proposed method is better in terms of robustness requirement than FIS because it is more resilient to salt and peppers noise (zonal sampling I 6% and zonal sampling II, 7% better); For JPEG compression, the proposed method is 6% better in zonal sampling I and 5% better in zonal sampling II. For low pass filtering, zonal sampling I is 12% better while 13 % better in zonal sampling II for the proposed method. For motion blurring attack, zonal sampling I and II are 9% better. However, FIS method performs slightly better when median filtering (6% in the average) and sharpening attacks (4% better than the proposed method) are applied. Even so, the correlation value of the proposed method can still be considered high which means, it is still robust against median filtering and sharpening attacks.

Table 7. Comparative result between FIS and the proposed enhanced watermarking method using DCT and zonal sampling

Type of Attack	FIS [26]	Proposed method	
		NCC	
	NCC	ZS1	ZS2
No Attack	1	1	1
JPEG Compression (50%)	0.8940	0.9568	0.9441
Salt & Pepper noise (1%)	0.6450	0.7061	0.7107
Low Pass Filtering	0.7483	0.8691	0.8801
Sharpening	1	0.9594	0.9634
Blurring motion [21 11]	0.9038	0.9892	0.9892
Median Filtering	0.7890	0.7305	0.7391

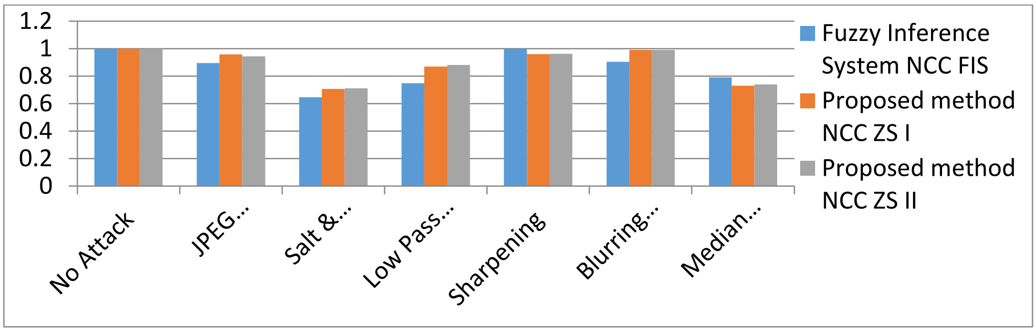

Figure 10. Comparative NCC results of the proposed method versus FIS using DCT in bar plots

In this second comparison, the proposed method is tested on gray level test image Mandrill of size 512*512 pixels with a watermark image of size 32*32 pixels, a logo taking the alphabets 'JNTU' as shown in Fig. 11(a-b).

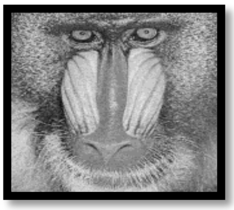

(a)

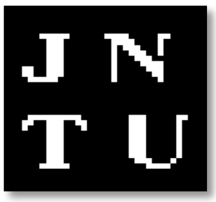

(b)

Figure 11. Original host image (a) Mandrill; (b) Watermark "JNTU"

Table 8 and Fig. 12 show the NCC values of the test image after watermark embedding process is performed using the proposed method which is compared with Neural Networks (BPNN and GRNN) [27]. The results indicate a detected perfect correlation for JPEG compressed watermarked images with quality factor q=90, and sharpening. Therefore, the proposed method is highly robust because there is a high correlation between the extracted watermark and the original watermark after different attacks.

However, the proposed method is vulnerable to median filtering against Back Propagation Neural Network (BPNN) (lesser robust 4% on the average) and about 37% lesser robust when salt and salt and pepper noise is applied to both BPNN and GRNN.

Table 8. Comparative result between Neural Networks and the proposed enhanced watermarking method using DCT and zonal sampling

Type of Attack	Neural Networks [27]		Proposed method	
	NCC		NCC	
	BPNN	GRNN	ZS I	ZS II
No Attack	0.9861	0.9907	1	1
JPEG Compression (90%)	0.9861	0.8904	1	1
Salt & Pepper noise (1%)	0.8760	0.8399	0.4890	0.4776
Low Pass Filtering	0.6510	0.4863	0.9818	0.9890
Sharpening	0.8182	0.8012	0.9744	1
Blurring motion [41 13]	0.5587	0.6892	0.9926	0.9926
Median Filtering	0.5189	0.3627	0.4785	0.4673

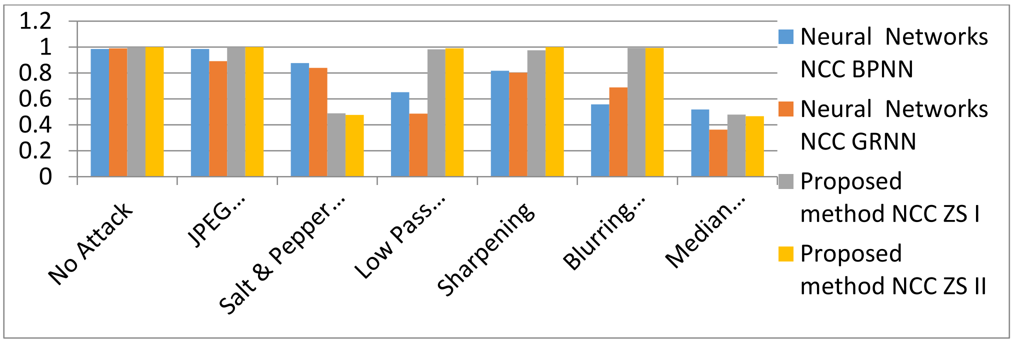

Figure 12. Comparative NCC results of the proposed method versus Neural Networks using DCT

3.3 Contour compression from watermarked image in frequency domain DCT using zonal sampling methods

In order to obtain the binary image from the attacked watermarked image Tools in (Fig. 13a), a threshold has been applied. The contour extraction is done through the SSPCE (Fig. 13b) while contour compression results were measured using the mean square error, peak signal-to-noise ratio and compression ratios. Table 9 shows the results of contour compression using Ramer method and zonal sampling I and II from attacked watermarked image Tools and Table10 for the Adaptive triangle method. The results obtained indicate visual representations of the compressed contours using Ramer method are shown in Fig. 14a and Fig. 14b while compressed contours using the Adaptive triangle method are shown in Fig. 15a and Fig. 15b.

Performed analysis and experiments for the analysed algorithms show that PSNR should be greater than 32 dB to obtain the expected compromise between compression ratio and quality of reconstruction. In the case of high threshold level, the contour details are eliminated and the level of introduced distortion will not be accepted. Compression ratio higher than 50 is within the acceptable target. This will apply to both the Ramer and Adaptive triangle method of contour compression.

a

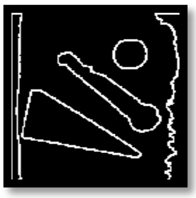

b

Figure 13. Host image Tools (a) Attacked watermarked host image (b) Extracted contours from attacked watermarked host image using SSPCE

3.3.1 Results in the frequency domain DCT using zonal sampling methods, SSPCE and Ramer contour compression method:

The following are the data gathered to recall, test image Tools' size is 256x256. In order to obtain the desired binary image of the attacked watermarked image Tools, four threshold values were used. Then by applying SSPCE, contours were extracted, followed by the visual representation of the acquired results from Table 9 of the compressed contour images from the attacked watermarked image Tools using the Ramer method and zonal sampling I and II respectively. In this manner, one could tell whether the data contained in the image are not damaged or altered but has maintained security and the binary image is still recognizable.

Table 9. Contour processing results in DCT using SSPCE, Ramer method and zonal sampling I & II

Thresholding	Zonal sampling I			Zonal sampling II		
	MSE	PSNR [dB]	CR [%]	MSE	PSNR [dB]	CR [%]
a) 0.1	0.000	Inf	54.137	0.000	inf	54.082
b) 0.6	0.031	56.026	69.960	0.031	51.040	70.045
c) 0.9	0.116	46.573	80.435	0.116	46.559	80.503
d) 1.2	0.153	45.189	82.124	0.153	45.198	82.141

Using DCT, it can be observed that as the threshold is increased, the PSNR value of the binary image decreases while compression ratio increases. From the results obtained in Table 9, zonal sampling I has a slightly better result than zonal sampling II, when it comes to the quality of the image during the approximation process using the Ramer method. The amount of distortion differs slightly to zonal sampling II. However, zonal sampling II has a better compression ability compared to zonal sampling I allowing a slightly higher amount of distortion.

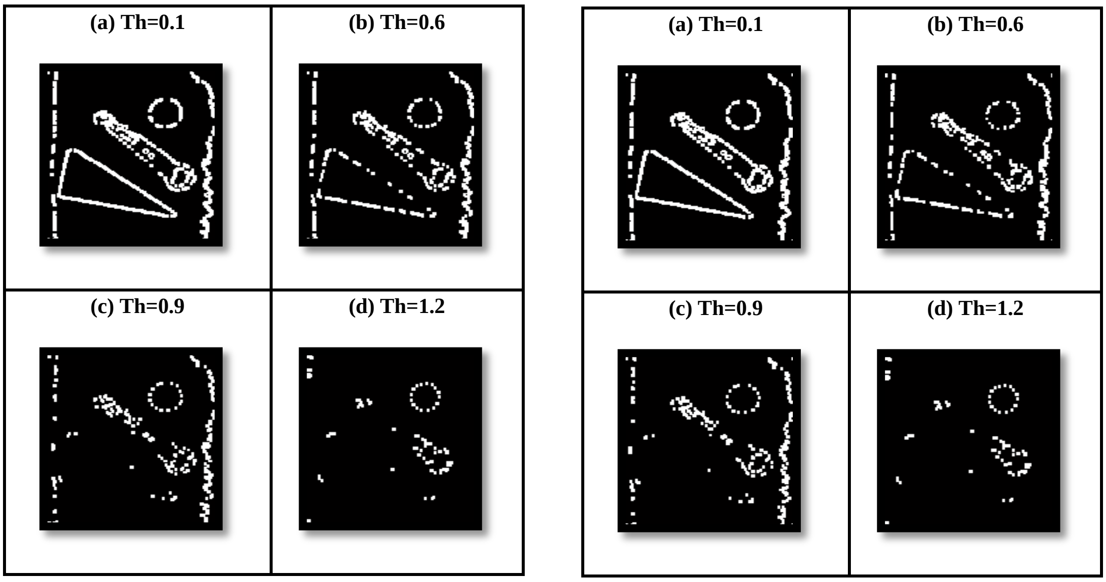

a *b*

Figure 14. Compressed contour of the watermarked image Tools using Ramer
a) zonal sampling I method b) zonal sampling II method

3.3.2 Results in the frequency domain DCT using zonal sampling methods, SSPCE and Adaptive triangle contour compression method:

The way to contour compression using the Adaptive Triangle has an identical process as the Ramer method. Meaning, a certain threshold is used in order to obtain the binary image from the attacked watermarked image, followed by contour extraction using SSPCE.

The difference between Ramer and the proposed Adaptive Triangle contour compression methods is that the first uses only one thresholding, while the latter uses a set of two thresholds at four given variables sets and a constant length (f) as shown in Table 10 for DCT. A time factor for in seconds is also included to measure its compression speed while distortion is measured by taking its Mean Squared Error, peak signal-to-noise ratio criterions to measure image quality after compression, and compression ratio (or bit per pixel).

In order to obtain the desired binary image of the test image Tools, four threshold values were used. As the threshold is increased, the PSNR value of the binary image decreases while compression ratio increases. From the results obtained, the Adaptive triangle method shows better results maintaining higher PSNR values compare with Ramer, both in zonal I and II. Although Ramer has shown higher compression per threshold, it has a lesser average compression ability (71.50% zonal sampling I and 71%,75% for zonal sampling II), Adaptive triangle method achieves a higher compression ability (76 % and 77% for zonal sampling I and II respectively) than Ramer even if the distortion of the image increased in every given double threshold. This proves that Adaptive triangle method produces good quality approximation with a fast-computational time. This also means that Adaptive triangle method for contour compression shows a 6% improvement when compared with Ramer.

Table 10. Contour compression results in frequency domain DCT using, SSPCE, Adaptive Triangle method and zonal sampling algorithm I & II

Method		MSE	SNR	CR[%]	Elapsed time (s)
Ramer		0.0183	17.38	69.47	9.89
Trapezoid		0.0184	17.36	69.88	9.44
Adaptive Triangle	zonal sampling I	1.42	53.37	72.72	0.174
	zonal sampling II	1.44	48.99	74.57	0.0643

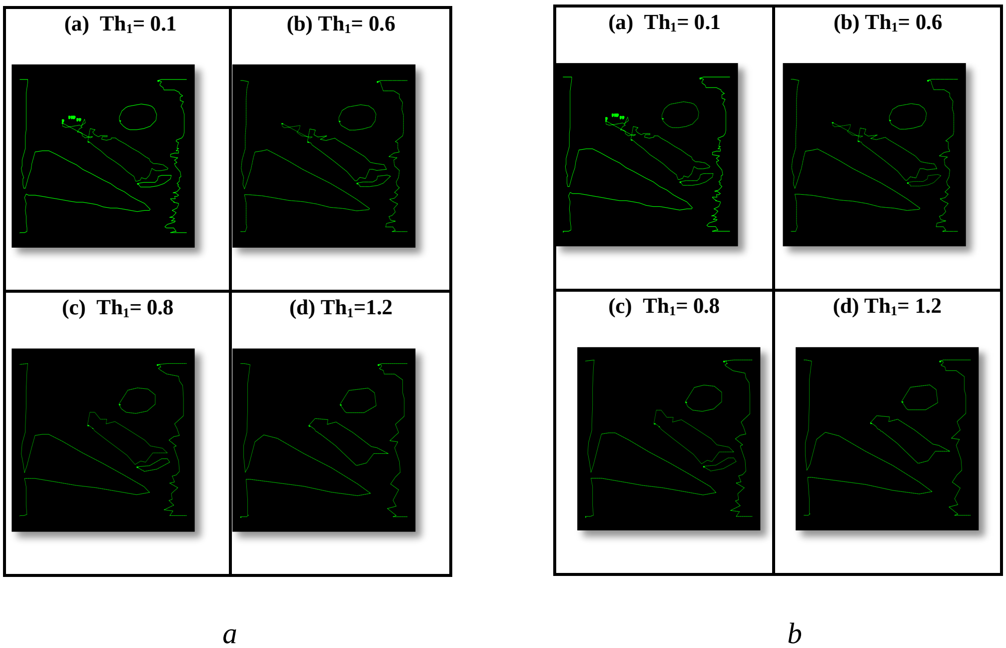

Figure 15. Compressed contour of the watermarked image Tools using Adaptive triangle method a) zonal sampling I method b) zonal sampling II

The results show that the proposed compression algorithm in DCT has slightly better PSNR and CR using zonal sampling algorithm II compared to zonal sampling algorithm I. The amount of distortion as per MSE is lower in ZS II thus giving a better quality compressed image. The elapsed compression time is also faster in ZS II as compared to ZS I.

3.4 Comparative results of the different contour compression methods against the proposed Adaptive Triangle method

In this section, further test is performed to compare and validate the compression abilities between Ramer, Trapezoid and the proposed algorithm [28] as shown in Table 11. Note that the image Tools with contour compression using the Adaptive triangle method is watermarked (UTHM FKEE) whereas Ramer and Trapezoid are not. This explains why higher MSE values on both zonal sampling I and zonal sampling II results are obtained.

The results show that the analyzed algorithm has a good extraction property and contour compression abilities with accepted quality compared with the binary image using threshold value in the case of Ramer and Trapezoid. It is seen that these two contour compression algorithms take more compression time while the method using Adaptive triangle is significantly faster compared with them for Tools image. The SNR is improved with the proposed algorithm compared to the binary images that use suitable threshold value only.

Measures				Zonal sampling I				Zonal sampling II			
Image	Thresholds		f	MSE	PSNR [dB]	CR [%]	TIME (s)	MSE	PSNR [dB]	CR [%]	TIME (s)
	Th1	Th2									
A	0.1	0.6	10	1.42	53.37	72.72	0.174	1.44	48.99	74.57	0.064
B	0.6	0.6	10	1.43	53.33	74.97	0.167	1.43	48.03	77.13	0.063
C	0.8	0.6	10	1.48	53.18	78.44	0.163	1.48	47.87	80.02	0.062
D	1.2	0.6	10	1.62	52.80	80.38	0.160	1.68	47.34	82.90	0.062

4 CONCLUSIONS

4.1 The proposed enhanced watermarking method

The watermarking method was tested and compared with other existing works using DCT and other combined techniques. From the experimental results gathered in the extraction process, the proposed enhanced watermarking method has a fidelity which is near identical to the original image as the PSNR values are always greater than 35 dB even when subdued to another image processing method prior to the extraction process. It is also robust against various attacks as the NCC values are 0.60 and above. Therefore, it can be concluded that using the proposed enhanced watermarking method using DCT with zonal sampling methods for embedding data passed the criterion of robustness and imperceptibility.

4.2 Contour extraction and contour compression techniques

A significant achievement from this paper is the combination of contour extraction using SSPCE and contour compression techniques from the attacked watermarked image which add value to image detection ability. Furthermore, it can be used with a minimum level of image distortion.

A method called Adaptive Triangle method for image compression is introduced. It is found that the short computational time of operations and good quality of approximation are the main advantages of the proposed algorithm. This gives usefulness in a wide application for contours where speed is necessary. It has a better compression ability compared with the Ramer and Trapezoid methods based on the experimental results.

5 REFERENCES

[1] J. C. Russ, The image processing handbook: Seventh Edition USA:CRC press, Taylor & Francis Group, 2016.

[2] A. J. Penrose and N. A. Dodgson, "Extending lossless image compression," University of Cambridge Computer laboratory Technical Report, p. 149, 2001.

[3] T. K. Araghi, A. B. A. Manaf, M. Zamani, and S. K. Araghi, "A Survey on Digital Image Watermarking Techniques in Spatial and Transform Domains," International Journal of Advances in Image Processing Techniques– IJIPT, vol. 3, pp. 16-10, 2016.

[4] S. S. A. Andrabi, "Sheenam “A Review: Information Hiding Using Watermarking Techniques”," SSRG International Journal of Computer Science and Engineering (SSRG-IJCSE)-EFES April, pp. 72-78, 2015.

[5] I. J. Cox, M. L. Miller, and J. A. Bloom, "Watermarking applications and their properties," in ITOC Las Vegas, Nevada, USA, 2000, pp. 6-10.

[6] T. A. Laskar and K. Hemachandran, "Digital Image Watermarking Techniques And Its Applications," in International Journal of Engineering Research and Technology, 2013.

[7] L. De Strycker, P. Termont, J. Vandewege, J. Haitsma, A. Kalker, M. Maes, et al., "Implementation of a real-

time digital watermarking process for broadcast monitoring on a TriMedia VLIW processor," IEE Proceedings-

Vision, Image and Signal Processing, vol. 147, pp. 371-376, 2000.

[8] N. Memon and P. W. Wong, "Protecting digital media content," Communications of the ACM, vol. 41, pp. 35-43, 1998.

[9] R. K. Singh, D. K. Shaw, and M. J. Alam, "Experimental Studies of LSB Watermarking with Different Noise," Procedia Computer Science, vol. 54, pp. 612-620, 2015.

[10] R. Joshi, L. Gagnani, and S. Pandey, "Image Steganography With LSB," International Journal of Advanced Research in Computer Engineering & Technology (IJARCET), vol. 2, pp. 228-229, 2013.

[11] P. Singh and R. Chadha, "A survey of digital watermarking techniques, applications and attacks," International Journal of Engineering and Innovative Technology (IJEIT), vol. 2, pp. 165-175, 2013.

[12] R. Kurban, H. Bozpolat, and F. Skuka, "Image Watermarking using DC Component of DCT," ICIT 2015 the 7th International Conference on Information and Technology pp. 344-348, 2015.

[13] A. K. Subudhi, K. Kabi, A. Subudhi, H. Patra, and J. B. Panda, "An enhanced technique for color image water marking using HAAR transform," in Electrical, Electronics, Signals, Communication and Optimization (EESCO), 2015 International Conference on, 2015, pp.1-5.

[14] C. K. Chui, An introduction to wavelets vol. 1. London, United Kingdom: Academic press, 2014.

[15] R. Dubolia, R. Singh, S. S. Bhadoria, and R. Gupta, "Digital image watermarking by using discrete wavelet transform and discrete cosine transform and comparison based on PSNR," in Communication Systems and Network Technologies (CSNT), 2011 International Conference on, 2011, pp. 593-596.

[16] A. Karmakar, A. Phadikar, B. S. Phadikar, and G. K. Maity, "A blind video watermarking scheme resistant to rotation and collusion attacks," Journal of King Saud University-Computer and Information Sciences, vol. 28, pp. 199-210, 2016.

[17] F. Ma, J. Zhang, and W. Zhang, "A blind watermarking technology based on DCT domain," in IEEE Transcript of the 2012 International Conference on Computer Science and Service System, 2012,pp.397-400.

[18] Majdi Farag Mohammed El Bireki, M. F. L. Abdullah and Ali Abdrhman M. Ukasha. “Adopting A Robust Watermarked Image Against Cyber Security Threats Using DCT and Ramer Method”, Fifth International

Conference on Intelligent Systems, Modelling and Simulation, 2014 IEEE, DOI 10.1109/ISMS.2014.160, pp. 295-300.

[19] S. Yuan and K.-B. Yu, "Zonal Sampling and Bit Allocation HT Coefficients in Image Data Compression," IEEE transactions on communications, vol. 34, pp. 1246-1251, 1986.

[20] A. A. M. Ukasha, "Methods of Contour Compression in Time and Spectral Domains," PhD Thesis, Faculty of Electrical Engineering, Automatics, Computer Science and Electronics, AGH-University of Science and Technology Poland, 2006.

[21] A. Dziech, "Contour Extraction and Compression-Selected Topics," in Mobile Robots: Perception and Navigation, S. Kolski, Ed., ed Germany/ ARS Austria: INTECH Open Access Publisher, 2007, pp.187-214.

[22] Majdi Farag Mohammed El Bireki, Ruqiya M Albahi Ali, Ali Abdrhman M. Ukasha and M. F. L. Abdullah. “An Adaptive-Triangle Method for Binary Image Contour Data Approximation.” Journal of Theoretical and Applied Information Technology. 2015. 81(2), pp. 343-348,.

[23] A. A. Ukasha, "A New Method for Contour Approximation Using Basic Ramer Idea," World Academy of Science, Engineering and Technology, International Journal of Electrical, Computer, Energetic, Electronic and Communication Engineering, vol. 5, pp. 33-38, 2011.

[24] A. A. U. A. B. Abdurrhman, "New Method for Contour Extraction & Compression using Ramer Algorithm & Wavelet Transform," in 6th European Computing Conference 2012, Advances in Computer Science, 2012, pp. 210-215.

[25] Majdi Farag Mohammed El Bireki, M. F. L. Abdullah, Ali Abdrhman M. Ukasha and Ali A. Elrowayati. “Digital Image Watermarking Based on Joint (DCT-DWT) and Arnold Transform.” International Journal of Security and Its Applications. 2016. 10(5). pp.107-118.

[26] Jagadeesh, B., Kumar, P. R. and Reddy, P. C. Fuzzy Inference System Based Robust Digital Image Watermarking Technique Using Discrete Cosine Transform. Procedia Computer Science. 2015. 46: 1618-1625.

[27] Jagadeesh, B., Jaganmohan, P. and AppalaRaju, M. HVS based Robust Image Watermarking in DCT Domain using Neural Networks. International Journal of New Trends in Electronics and Communication (IJNTEC). 2013. 1(2): 5-9.

[28] Ukasha, A. A. An Efficient Spatial Domain Methods & Wavelet Transform for Contour Compression. International Conference on Artificial Intelligence and Image Processing (ICAIIP). (UAE).2012.pp.225-229.

إستخدام تحويلة *DCT* للصور لتحسين جودة مخطط العلامة المائية إعتماداً علي خوارزمية أخذ العينات مع تطبيق أساليب إستخراج و ضغط الحدود بأستخدام تقنيات RAMER AND ADAPTIVE TRIANGLE

مجدي فرج البريكي[1*]، علي عبد الرحمن عكاشة[2]، جمال علي دوفان[3]، محمد فايز عبد الله[4]

[1] قسم الهندسة الكهربية و الالكترونية، المعهد العالي للعوم والتقنية تامزاوة ليبيا، *majdi_elbreki@yahoo.com*
[2] قسم الهندسة الكهربية و الالكترونية، جامعة سبها ليبيا، *ali.ukasha@sebhau.edu.ly*
[3] قسم الهندسة الكهربية و الالكترونية، جامعة غريان ليبيا، *jardgsm@gmail.com*
[4] كلية الهندسة الكهربية و الالكترونية، جامعة تون حسين عون ماليزيا، *faiz@uthm.edu.my*

لخص

تقترح هذه الورقة مخططًا للعلامة المائية يعتمد على تحويل DCT للصور وخوارزمية أخذ العينات النطاقية المحددة. بالمخطط المستخدم يتم الإحتفاظ بمعاملات تحويل LPF وHPF في منطقة هندسية معينة من الصورة الأصلية. يتم تعيين وتحديد وضبط باقي المعاملات على قيمة صفر (0) ، ويتم تحديد الكمية ونقلها إلي مكان تضمين العلامة المائية. من أجل اختبار قوة ومتانة العلامة، يتم تنفيذ بعض الهجمات. ومع ذلك ، قبل عملية استخراج العلامة المائية ، سيتم إخضاع الصورة ذات العلامة المائية المهاجمة إلى طرق معالجة الحدود بإستخدام خوارزمية إستخراج الحدود أحادية الخطوة ، وخوارزميات Ramer و Adaptive Triangle لضغط الحدود. ستساعد الطريقة المقترحة لضغط الحدود في تعزيز التعرف على الصور والأمان وخاصة عندما يكون الوقت (السرعة) عاملاً أساسيًا. أظهرت النتائج أن طريقة العلامة المائية المقترحة قوية وآمنة ضد هجمات معالجة الإشارات / الصور المختلفة بقيم PSNR تبلغ حوالي 35 ديسيبل مع قيم NCC من 0.60 وما فوق. بالإضافة إلى ذلك ، تشير النتائج التجريبية من ضغط الحدود إلى أن طريقة Adaptive Triangle المقترحة لها نسبة ضغط عالية دون تشويه مرئي كبير.

الكلمات الدالة:
العلامة المائية.
الحدود.
تقنية DCT.
تقنية Ramer.
تقنية Adaptive Triangle.

: البريد الإلكتروني للباحث المراسل *majdi_elbreki@yahoo.com*